

Late-time Kerr tails revisited

Lior M. Burko^{1,2} and Gaurav Khanna³

¹ *Department of Physics, University of Alabama in Huntsville, Huntsville, Alabama 35899, USA*

² *Center for Space Plasma and Aeronomic Research,*

University of Alabama in Huntsville, Huntsville, Alabama 35899, USA

³ *Department of Physics, University of Massachusetts – Dartmouth, N. Dartmouth, Massachusetts 02747, USA*

(Dated: draft of February 18, 2019)

The decay rate of late time tails in the Kerr spacetime have been the cause of numerous conflicting results, both analytical and numerical. In particular, there is much disagreement on whether the decay rate of an initially pure multipole moment ℓ is according to $t^{-(2\bar{\ell}+3)}$, where $\bar{\ell}$ is the least multipole moment whose excitation is not disallowed, or whether the decay rate is according to t^{-n} , where $n = n(\ell)$. We do careful 2+1D numerical simulations, and find that the tails decay according to the former, for the case that has become the testbed of such studies, specifically an initially pure $\ell = 4$ multipole on a Boyer–Lindquist time slice. We then discuss some of the causes for possible errors in 2+1D simulations, demonstrate that our simulations are free of those errors, and argue that conflicting past results may be attributed to them.

PACS numbers: 04.70Bw, 04.25.Nx, 04.30.Nk

I. INTRODUCTION AND SUMMARY

The late-time tails of black holes have been studied in much detail since Price’s seminal work [1]. The formulation of the problem is a straightforward one: place an observer in a circular orbit around a black hole, and have her measure at late times a generic perturbation field, that had compact support at some initial time. It is generally accepted that the observer measures the late-time perturbation field to drop off as an inverse power law of time, specifically as t^{-n} . It is the value of n that has been controversial in the literature, with some conflicting results reported.

In the case of a Schwarzschild black hole, $n = 2\ell + 3$, where ℓ is the multipole moment of the initial perturbation field. Namely, if the initial (compactly supported) perturbation field has the angular dependence of Y_ℓ^m , the angular dependence remains unchanged (“spherical harmonics are eigenvectors of the Laplacian operator”), and the decay rate of the field is governed by the ℓ value of the initial perturbation. These results remain unchanged also for a Reissner–Nordström black hole [2] (including the extremal case [3]), that like the Schwarzschild black hole is spherically symmetric. Notably, a generic perturbation is a linear superposition of ℓ -modes, so that the tail is dominated by the slowest damped mode, or by the lowest value of ℓ .

For rotating black holes conflicting values of n have been reported. Obviously, the observer measures a well defined decay rate. The correct answer to the question of the value of n was described in [4]: the late-time field decays according to the same rule as in the spherically-symmetric case, namely according to $t^{-(2\bar{\ell}+3)}$, where $\bar{\ell} = m$ if $\ell - m$ is even, and $\bar{\ell} = m + 1$ if $\ell - m$ is odd, independently of the initial value of ℓ . The reason for this decay rate is that spherical harmonic modes do not evolve independently on the background of a rotating black hole (“spherical harmonics are *not* eigenvectors of

the Laplacian operator”). Starting with an initial value for ℓ , infinitely many other ℓ modes are excited, respecting only the dynamical constraints ($\ell \geq s$, where s is the spin of the field, and $\ell \geq |m|$) and the equatorial symmetry of the initial data (such that even and odd modes do not mix).

The results of this Paper are in full accord with the conclusions of [4]. This paper’s motivation is to explain some of the historical discrepancies, in what we believe is an illuminating manner. Specifically, finding the reasons for the controversy in the literature teaches us important lessons. In particular, we will consider two results, conflicting both with each other and with the results of [4] and of this paper: the numerical results of [5], and the analytical model of [6]. More precisely, we consider the simplest case for which there is a disagreement in the literature, specifically the case of a massless scalar field ($s = 0$) perturbation of a Kerr black hole, with initial $\ell = 4$ and $m = 0$. For this case, the late time tail drops as t^{-3} , because the monopole ($\ell = 0$) mode of the scalar field can and is excited, and this mode’s drop off rate obeys the $t^{-(2\ell+3)}$ rule. The (numerical) results of [5] suggest a drop off rate of $t^{-5.5}$, and the Poisson analytical model (of a globally weakly curved spacetime) predicts a drop off rate of t^{-5} if carried over to the Kerr case [6]. Poisson’s conclusions are identical to the results of [7].

In the case of [5], we attribute the (numerically stable!) result of a drop off rate of $t^{-5.5}$ to an intermediate tail being misidentified as an asymptotic tail. As we show, the traditional representation of the tail in a log–log plot of the field as a function of time is susceptible to lead to an “optical illusion,” that may support this misidentification. Specifically, we show what may be interpreted as a tail falling off as $t^{-5.5}$, similar to what is found in [5], except that if the integration is carried on further in time the intermediate behavior is taken over by the true asymptotic behavior, or a tail falling off as

t^{-3} . The reason [5] mistook an intermediate tail for an asymptotic one is that [5] chose parameters that make it harder to distinguish the two using the crude tools used in [5]. Specifically, we show that the farther out the initial pulse, the longer the intermediate tail. Reference [5] chose the initial pulse very far out, which resulted in a protracted intermediate tail. While this choice made the problem severe enough, it was even further exacerbated by making the initial pulse outgoing and by taking the Kerr parameter $a/M = 0.9999$. Either choice makes the beginning of the tail regime postponed. As the integration time in [5] is rather short, we conclude that the tail analyzed in [5] is an intermediate one, and that if the integration time were longer, [5] too would have found a t^{-3} tail. (In view of our argument below, we comment that the code of [5] was fourth order angularly, which we find to be satisfactory for the relatively short runs done by [5].)

How can one then avoid misinterpreting intermediate tails as asymptotic ones? We provide a criterion, that we believe can be used for the identification of the asymptotic tail. By our criterion, a tail is asymptotic if the local power index [8] is linear in t^{-1} both locally and globally, in a sense that we make precise.

In the case of [6], we explicitly follow the proposal of Poisson, and evolve initial data that are a pure spherical harmonic mode with respect to “spherical” coordinates, not the Boyer–Lindquist coordinates, that are “spheroidal” in the language of [6]. According to [6], such initial data should lead to a very curious time evolution, in which exact cancellations allegedly lead to modes that evolve not according to the $t^{-(2\ell+3)}$ rule, but rather according to an intricate rule that “remembers” the field’s initial multipole *even though the field is linear*. Specifically, starting with $\ell = 4$ and $m = 0$, Poisson predicts the asymptotic tail to drop off as t^{-5} . In [6], such time evolution is demonstrated in a globally weak–curvature spacetime (that has no symmetries), and it is conjectured that such behavior is carried over to the case of a Kerr black hole. We show that this conjecture is not realized: instead, the evolution is according to the conclusions of [4], and the drop off rate is according to t^{-3} .

Very recently, Gleiser, Price, and Pullin (henceforth GPP) have proposed a theoretical model that expands the wave equation in (even) powers of the black hole’s spin rate a [9]. The advantage of the GPP approach is that the zeroth order wave operator is identical to the spherically–symmetric operator, so that it can be solved numerically using a simple 1+1D code. Each iteration in the GPP approach gives the field to the next order in a^2 , using the field of the previous iteration as the source term of a spherically symmetric wave operator. GPP argue that their approach is superior to the 2+1D approach, because it frees the numerics from the subtleties of the 2+1D simulations, and because the 1+1D numerics are inherently more reliable. We totally agree with these claims, yet disagree with the conclusions of GPP, according to which the tails predicted by [7] are found.

The GPP argument implies that delicate cancellations exactly cancel not only the leading tail term (in an expansion in t^{-1}), but also the leading subdominant mode [10] (for an initial $\ell = 4$; for other initial choices more subdominant modes may need to be cancelled). GPP further argue that turning off the coupling term at very late times destroys the exact cancellation, so that the tail returns to the “naive” decay rate. It is quite remarkable that even if this is done at extremely late times, so that the hexadecapole field is much smaller than the monopole field, it still does not lose its ability to exactly cancel out its two leading terms (in t^{-1}).

Notably, GPP imply that different slicing conditions may be responsible for the apparently conflicting results of numerical simulations. Indeed, in [4] the slicing condition was that associated with ingoing Kerr coordinates, in [11] the slicing was that of the Kerr–Schild coordinates, and in [5] Boyer–Lindquist slicing was used. GPP argue that the translation of an initially pure $\ell = 4$ mode, say, in some other slicing condition (e.g., ingoing Kerr or Kerr–Schild) into Boyer–Lindquist slicing results in a mixed state of modes for the Boyer–Lindquist slicing, and the existing lower ℓ (specifically, the quadrupole and monopole) modes on the initial time slice are the ones responsible for the tail structure. According to GPP, among all slicing conditions the Boyer–Lindquist one is special, as only in this slicing an initial pure $\ell = 4$ mode leads to a tail of t^{-5} , and in all other slicing conditions an initially pure $\ell = 4$ mode leads to a t^{-3} tail. We disagree with this viewpoint, as we find that also for Boyer–Lindquist slicing the tail decays like t^{-3} . We argue that the numerical results of [5] were misinterpreted, and in fact do not support the claim for a t^{-5} tail.

We argue that careful 2+1D simulations should obtain the correct Price tail, and we contend that our numerics are done with sufficient care. Any suggestions why GPP obtain different tails than we do would be mere speculations, so we refrain from making them. We believe that the GPP strategy should have led to tails, identical to those proposed here.

The essence of the case we make is as follows: we first show that our tails are numerically convergent, and that the field we obtain is a physical field, and not evolved numerical noise. Then, we bring evidence that the tail we see is indeed the asymptotic one, and not an intermediate tail. Lastly, we expand our field in powers of a^2 , and study the behavior of each power in this expansion. We bring evidence that each order in a^2 drops at late times according to $t^{-(2\bar{\ell}+3)}$, where $\bar{\ell}$ is the least value allowed dynamically that is consistent with the equatorial symmetry. We are hopeful that this Paper may put some order in a confused state of affairs, in which the literature includes side by side correct results and incorrect ones, without a proper explanation of the incorrect ones.

The organization of this paper is as follows. In Section II we discuss the reliability of the 2+1D approach in calculating tails, and how carelessness can result in an incorrect value for the field. In Section III we discuss the

decomposition of the monopole projection of the tail in powers of a^2 , and in Section IV we discuss one possible pitfall that can cause a correct field be misinterpreted. In Section V we analyze a pure mode in “spherical” coordinates [6], and show that it leads to the same tail decay rate as in “spheroidal” coordinates.

II. RELIABILITY OF THE 2+1D CODE

The solution of the Teukolsky equation in 2+1D is delicate and sensitive, and can lead to qualitatively wrong results if proper care is not taken. In Section IV below we show that even when the numerically computed field is the correct one, careless interpretations may lead to incorrect conclusions. In this section we first demonstrate how carelessness may lead to qualitatively wrong behavior of the solution, and then we demonstrate the reliability of the approach when proper care is taken.

A. Second order angular differentiation

The standard of scientific computation in the finite difference approach has been second order algorithms for many years. Indeed, second order convergence typically implies the solution is both consistent and stable to a practical level, so that the solution is accurate enough without having to reduce the typical grid spacing to extremely low levels that would make the code too costly computationally. Normal application of the Dahlquist theory (extended to PDEs) then means that if the discrete formula approximating the differential equation has locally a positive order of accuracy (convergence), and that if numerical errors do not grow unboundedly (stability), then the solution is convergent, in the sense that as the grid spacing goes to zero, the solution would approach the correct one. As we show below, the tail problem involves the Dahlquist theory with a twist.

Early codes to calculate the late-time Kerr tail were therefore designed to be second-order in all coordinates, i.e., temporally, radially, and with respect to the angular coordinate θ [12]. (In the 2+1D approach the field is decomposed into φ modes, so that one does not have numerical derivatives with respect to φ .) While this approach seems very natural, it can mislead into qualitatively wrong solutions. Consider first a Schwarzschild black hole, excited by an azimuthally symmetric ($m = 0$) field with $\ell = 4$. The decay rate of the Price tail is incontrovertible in this case: as the background is spherically symmetric, spherical harmonic modes evolve independently, and the decay rate is therefore t^{-11} . Indeed, 1+1D codes readily verify this result.

The numerical solution with a second-order 2+1D numerical code may lead however to the erroneous conclusion that the decay rate is t^{-3} : in Fig. 1 we show the late-time field as a function of time for three choices of the angular grid spacing, and for fixed radial and tem-

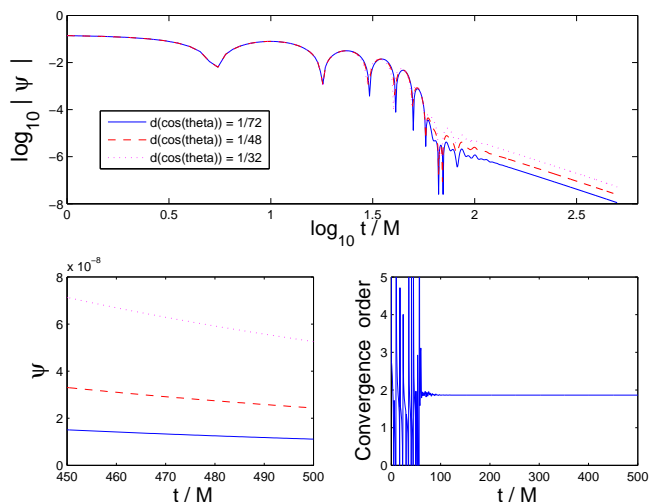


FIG. 1: Convergence tests for Schwarzschild initial data with the second-order code. Upper panel and lower panel on the left: the full field (evaluated at $\theta = \pi/2$) for three different angular resolutions ($\Delta \cos \theta = 1/72$ (solid), $1/48$ (dashed), and $1/32$ (dotted)) as a function of time. The lower panel on the right is the convergence order as a function of the time at $r_*/M = 25$. The initial data are for a Schwarzschild black hole ($a/M = 0$), and are a gaussian centered at $r = 25M$ with width $4M$. The radial resolution is $\Delta r = M/32$, and the temporal resolution is chosen to be $\Delta t = \Delta r/2$, which satisfies the Courant condition. The initial data are a pure multipole with $\ell = 4$.

poral grid spacings. As can be readily inferred from the upper panel in Fig. 1, the decay rate is t^{-3} , which is definitely wrong. The origin of this wrong result is indicated in the same figure: the field values themselves reduce considerably in amplitude under refinement of the grid (almost as the second power of the ratio of the grid parameters). The signal seen is therefore not the physical field, but an evolved numerical noise (“leakage of multipoles”). Our interpretation is that while the physical signal indeed drops like t^{-11} , it is swamped by the evolved numerical noise, which has a monopole component. The latter drops like t^{-3} , so that any very long time evolution must be dominated by numerical noise. Refinement of the grid parameter can postpone the numerical-noise dominated regime, but cannot utterly eliminate it: refinement of the grid parameter reduces the level of the numerical noise, so that if the grid is fine enough, the noise level at a particular value of the time reduces to below the level of the physical field. However, as the former drops more slowly than the latter, at very late times the field is dominated by numerical noise (see Fig. 2 below).

Here enters the twist on the Dahlquist theory: the numerical noise does not grow unboundedly. In fact, it even drops quadratically with the grid spacing, and drops with time. It does so, notwithstanding, slower than the physical signal, so that the signal may be dominated by numerical noise even though the regular Dahlquist criteria

are apparently satisfied.

B. Sixth order angular differentiation

While a second order code may in principle be sufficient to see physical tails (for very fine grids), an alternative approach is to increase the order of the angular differentiation. We first show how the same initial data and grid resolutions lead to qualitatively different results in Schwarzschild, and then we discuss Kerr.

Figure 2 shows the sixth order convergence of the field, for the same parameters that were shown in Fig. 1 with the second order code. The field is not made of evolved noise (“leakage of multipoles”), as it clearly converges to a non-zero value under grid refinement. Notably, the field’s amplitude even *increases* slightly under grid refinement. The hallmark of noise signals is that their amplitude *decreases* under grid refinement, as is indeed evident in Fig. 1. Most importantly, the Price tail drops as t^{-11} , as it should. We emphasize that these conclusions are true up to some maximal time value. For longer times the residual monopole noise, that drops slower than the physical field, will inevitably dominate. Simple extrapolations reveal that the signal noise will dominate over the physical signal for $t \gtrsim 4,380M$ for our choice of angular resolution. Longer evolutions than that will be dominated by noise evolution. As noted above, it is not difficult to separate the physical signal regime from the noise signal regime by doing global convergence tests. It is therefore crucial *for any tail simulation* that convergence tests are done throughout the entire computational domain, and not limited just to short integration times (despite the temptation to save computer time — e.g., see [5]).

In Fig. 3 we demonstrate the sixth order angular convergence of Kerr evolutions. This figure summarizes the main parts for our claim that our tail results are reliable: The code is convergent to a non-zero value, and even increases in magnitude with grid refinement (so that the signal seen is not an evolved noise signal), and the convergence order is global, throughout the computational domain. Notice that in Fig. 3 we study the convergence with the monopole projection of the total field. This projection is more sensitive to the created and evolved monopole numerical noise than the full field, say, as we can test its convergence also at times earlier than the instant the monopole dominates the total field for the first time. Figure 6 depicts the (L_2 norm of the) full field and its monopole projection. The parameters are chosen so that intermediate tails are minimized, so that computation time is used efficiently. The monopole projection amplitude is many order of magnitudes higher than typical “multipole leakage” noise levels (cf. with Fig. 2). Indeed, it is the result of physical multipole excitations, not noise generation. Below, we also bring evidence that the observed tail is indeed asymptotic, so that we are not misled by an intermediate tail masquerading as an

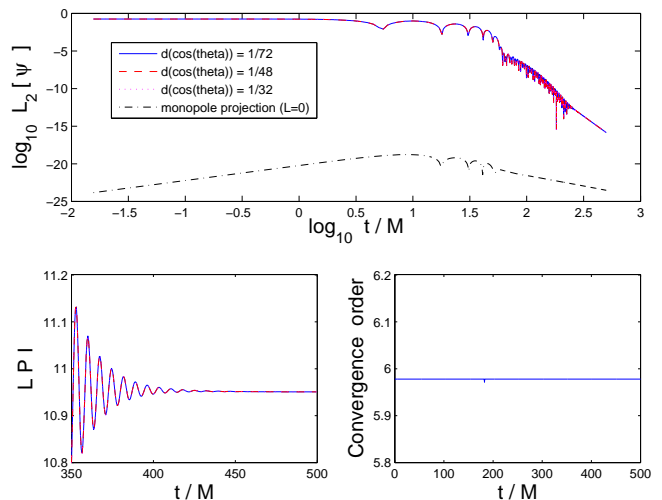


FIG. 2: Same initial data and resolutions as in Fig. 1 for the sixth order code. The upper panel shows the L_2 norm for the full field (integrated over a sphere at $r_* = 25M$) in three resolutions. The three curves are nearly indistinguishable on this plot’s scale. The upper plot also shows the monopole projection of the field, which is pure evolved numerical noise for resolution of $\Delta \cos \theta = 1/64$. This figure also shows the tails local power index as a function of time (lower left) and the convergence order of the three resolution shown on the upper panel (lower right).

asymptotic one.

III. THE TAIL IN AN a^2 EXPANSION

GPP argue that when expanded in powers of a^2 , the tail would be at $O(a^4)$, and that this part of the tail drops as t^{-5} . In this Section we confront these claims with accurate 2+1D results. When a mode P_n exists at any iteration order (in a^2), at the next iteration three modes will result: P_{n-2} (if $n-2 \geq 0$), P_n , and P_{n+2} . The mode excitation scheme is shown in Fig. 5. In the GPP approach, this behavior comes about because of the term $\sin^2 \theta \times P_n(\cos \theta)$ appearing in the source term (see [9] for detail). This way, starting with a pure $\ell = 4$ mode, there is just one way to create a monopole field at $O(a^4)$, but three ways to create a monopole field at $O(a^6)$. It has been suggested that the GPP results deviate from 2+1D numerical results because GPP did not include the monopole field to $O(a^6)$ (or higher) in their analysis: if the monopole field to $O(a^4)$ indeed falls like t^{-5} as predicted by GPP, but to $O(a^6)$ (or higher) falls like t^{-3} , the latter will dominate at late time even though it is at higher order in a^2 (and even for small values of a). Our results below show this is *not* the reason for the apparent discrepancy. Already at $O(a^4)$ we find the monopole field to drop like t^{-3} .

Specifically, we write the monopole projection of the

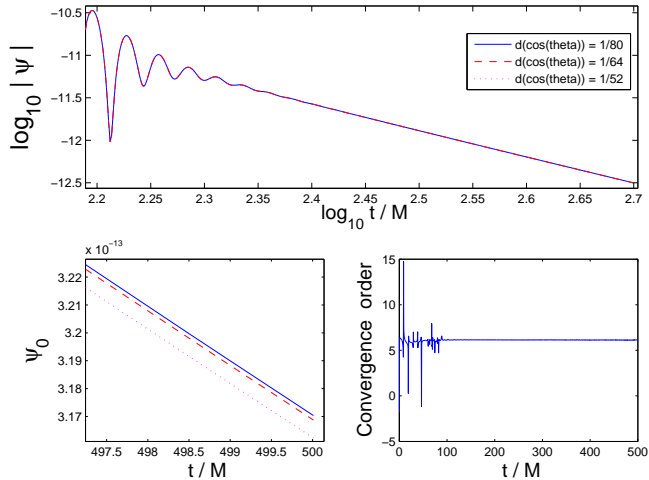


FIG. 3: Same as Fig. 1 for the monopole projection of the full field using the sixth order code for Kerr. The angular resolutions are $\Delta \cos \theta = 1/80$ (solid), $1/64$ (dashed), and $1/52$ (dotted). The initial data are an outgoing Gaussian pulse located at $r_* = 25M$ with width of $4M$ with compact support on the Boyer–Lindquist $t = 0$ hypersurface of a Kerr black hole with $a/M = 0.995$. The initial multipole is a pure Boyer–Lindquist $\ell = 4$. The radial resolution is $\Delta r = M/50$, and the temporal resolution is chosen so that $\Delta t = \Delta r/2$.

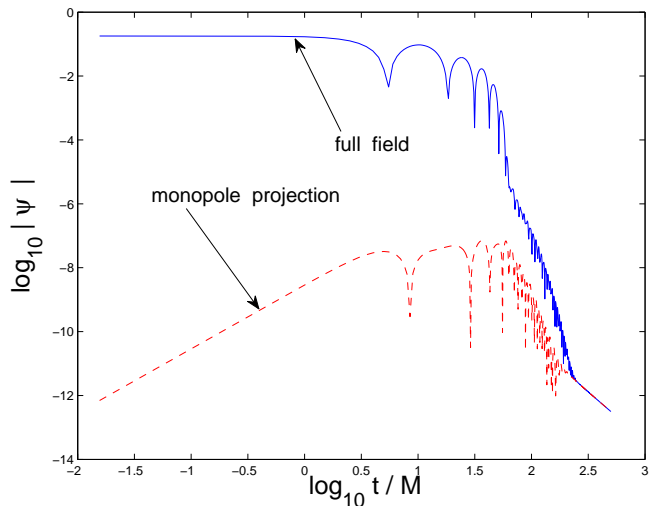


FIG. 4: Same as Fig. 3. Shown are the L_2 norm of the full field (solid curve) and the field’s monopole projection (dashed curve). For both, the angular resolution is $\Delta \cos \theta = 1/72$ and the radial resolution is $\Delta r = M/32$. The temporal resolution is chosen so that $\Delta t = \Delta r/2$.

field ψ_0 as an expansion in the spin parameter a :

$$\psi_0 = \sum_{n=0}^{\infty} C_n(t) \times a^n. \quad (1)$$

According to GPP only even powers of a have non-zero coefficients, and $C_0(t) = 0 = C_2(t)$, so that the first non-

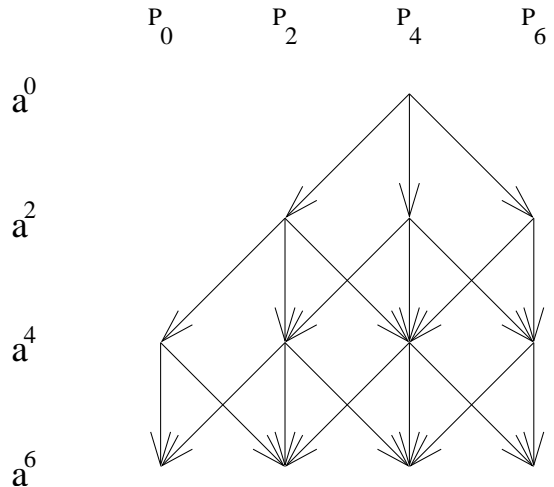


FIG. 5: The mode coupling schematics: at each iteration in a^2 in the GPP approach, each ℓ modes excites three modes, specifically $\ell - 2, \ell$, and $\ell + 2$. The initial data are purely hexadecapolar. We show only modes up to $O(a^6)$ and $\ell = 6$.

zero coefficient is $C_4(t)$. GPP then argue that $C_4(t) \sim t^{-5}$ (for a pure Boyer–Lindquist initial mode with initial $\ell = 4$).

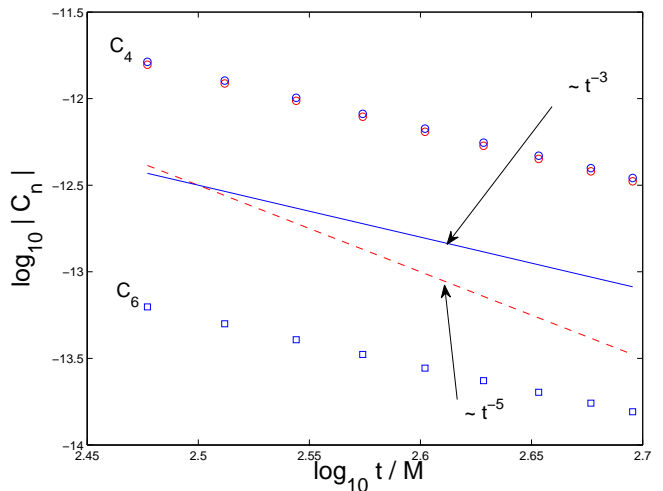


FIG. 6: The coefficients $C_4(t)$ and $C_6(t)$. The two sets of data points (\circ) corresponding to $C_4(t)$ relate to fits to the ansatz $\psi(t) = C_4(t) a^4$ (slightly higher) and $\psi(t) = C_4(t) a^4 + C_6(t) a^6$. The coefficients $C_6(t)$ are represented by \square . We also show two reference lines, with slopes of -3 (solid) and of -5 (dashed).

We can find the coefficients $C_n(t)$ from a 2+1D simulation in the following way: We take the monopole projection value of the field in the tail regime at a fixed value of time for various a values. In practice, we considered a values in the range $0.05 \leq a/M \leq 0.995$. We then fit the data to two ansatzs: first, to $\psi_0 = C_4 a^4$, and second, to $\psi_0 = C_4 a^4 + C_6 a^6$. That is, we obtain the numerical val-

ues of the coefficients C_n for that particular value of the time. The fit is very good: we get the squared correlation coefficient to be better than 0.999. We then repeat for a number of time values, so that we have $C_4(t)$ and $C_6(t)$. We can then find the time dependence of $C_4(t)$ and of $C_6(t)$. Our results are shown in Fig. 6. Both $C_4(t)$ and $C_6(t)$ drop off as t^{-3} . We emphasize that the raw data are taken from Fig. 3: the data converge at sixth order angularly, and is the physical signal, not an evolved noise signal.

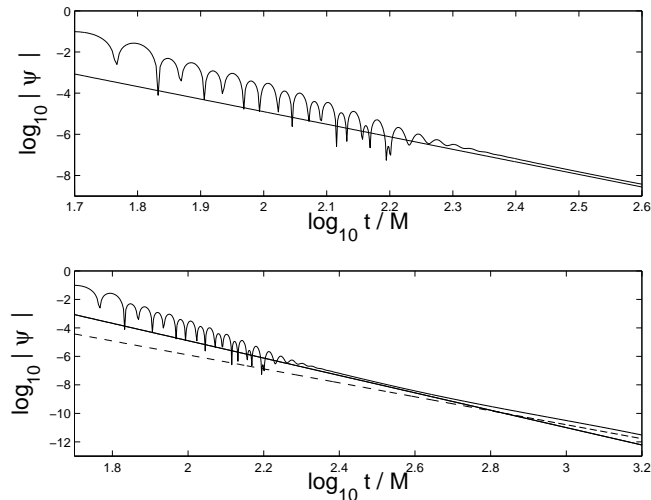


FIG. 7: Solid curve: the full field. Solid reference line has a slope of 6.1. Dashed reference line has a slope of 4.9. Initial data were a Gaussian with $\ell = 2$. It was centered at $30.0M$ with a width of $4M$. The grid resolution was: radial resolution $\Delta r = M/20$ and angular resolution $\Delta \cos \theta = 1/32$. Here, $a/M = 0.8$.

IV. OPTICAL ILLUSION

When having asymptotic phenomena, it is crucial that the observations are made in the asymptotic regime. In Fig. 7 we show the field starting at the same times, but extending to two different values of time. In the upper panel extending to $t = 400M$, and in the lower extending to $t = 1600M$. In the upper panel we show a reference line with a slope of 6.1. One may be tempted to deduce from the seemingly two parallel curves at late times that the asymptotic slope of the field is 6.1. In the lower panel of Fig. 7 we show the same field and the same reference line, but we add another reference line, with slope of 4.9. Extending the integration time, it now appears that the asymptotic slope is 4.9. Which is it? 6.1 or 4.9? The correct answer is 3. The slope of 5.5 reported on in [5], we believe, is just this effect: the field's decay rate was determined in [5] not in its true asymptotic regime.

In Fig. 8 we show the full field up to $t = 500M$ and to $t/M = 2950$. At first we show a reference curve with slope of 5.5, and then increase the integration time, and

show both the first reference curve, and a new one with slope of 3.0. In particular, if we were uncareful we could report on a tail index of 5.5 like that of [5]. Continuing the simulation, however, we find the true asymptotic tail, with a tail index of 3, as expected.

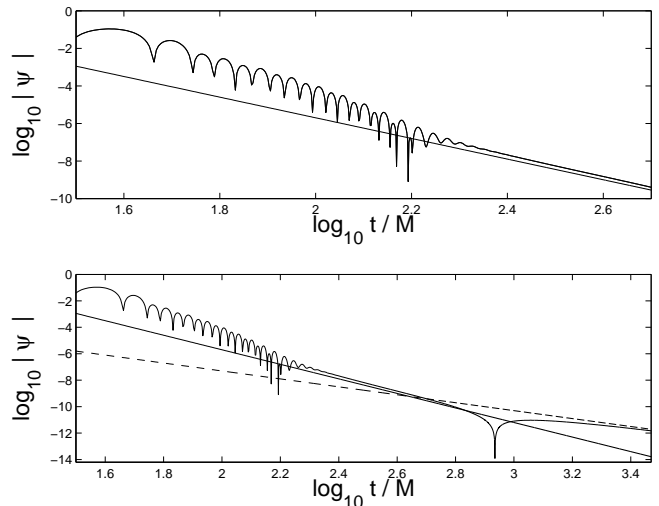


FIG. 8: Solid curve: the full field. Solid reference line has a slope of 5.5. Dashed reference line has slope of 3. Initial data were a Gaussian with $\ell = 2$. It was centered at $17.5M$ with a width of $4M$. The grid resolution was: radial resolution $\Delta r = M/20$ and angular resolution $\Delta \cos \theta = 1/32$. Here, $a/M = 0.8$.

The arbitrariness of the decay rate, as determined from intermediate time segments, is further exemplified in Fig. 9, which shows the field for a number of different choices of r_0 , the center of the initial pulse. The closer the pulse is to the black hole, the sooner the true asymptotic tail appears. Conversely, pushing the initial pulse outwards, we protract the intermediate tail regime, and can make it as long as we want: it is fully controllable. The choice of the length of the intermediate tail also affects its decay rate determination. We therefore see that not only is such a decay rate meaningless, it is also directly manipulable. The important lesson here, reflecting on the claims made in [5], is that a distant initial pulse makes it harder to see the asymptotic tail, and it would require longer time evolutions. In [5], the initial pulse was chosen at $r_0 = 100M$, which would make the intermediate tail very protracted indeed.

Figure 10 explains the broken power-law behavior we see in Fig. 7, and also why neither is the true asymptotic field: Up to $t \sim 500M$ the field is dominated by the dipole ($\ell = 2$) mode, and at later times it is dominated by the monopole ($\ell = 0$). Notice, that even the seemingly constant slope in the lower panel of Fig. 7 does not represent the asymptotic behavior of the field, as is clear from Fig. 10. The “optical illusion” effect is not a result of mode mixing: it appears in each mode separately. Indeed, in the $\ell = 0$ mode what may appear as a straight segment (on the log-log plot of Fig. 10) is

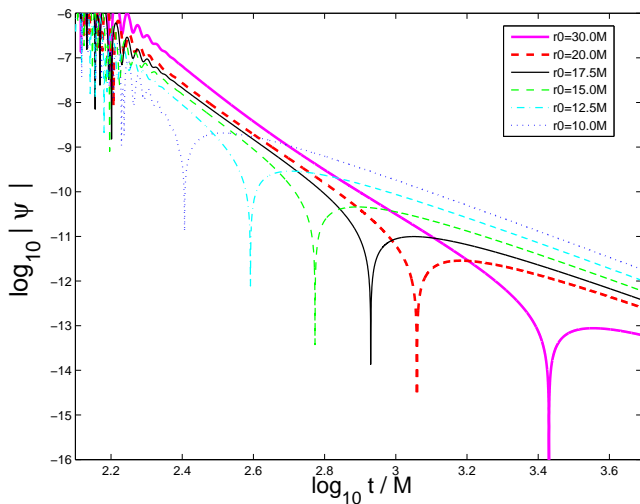


FIG. 9: Effect of varying the location of the initial pulse. In all these runs, initial data was a Gaussian of width $\lambda = 4M$, with $\ell = 2$, and $a/M = 0.8$. The grid resolution was: 0.05 (r) \times 0.03125 (angle). The curves shown and the corresponding value for r_0 , the center of the initial data gaussian, are: dotted curve: $r_0 = 10M$, dash-dotted curve: $r_0 = 12.5M$, dashed curve: $r_0 = 15M$, solid curve: $r_0 = 17.5M$, dashed thick curve: $r_0 = 20M$, and solid thick curve: $r_0 = 30M$. All data are extracted at $r = 17.5M$.

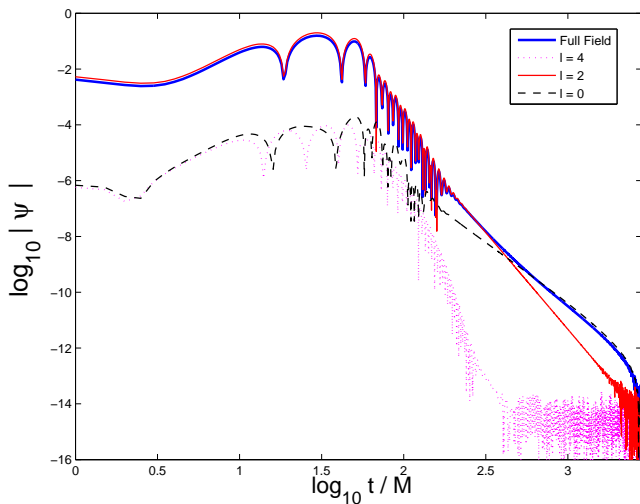


FIG. 10: Same data as in Fig. 7. The full field is decomposed into the Boyer–Lindquist multipole modes.

curving if the integration time is extended. But when we combine the two separate optical illusions of the $\ell = 2$ and $\ell = 0$ modes, we may get a broken power-law as in the lower panel of Fig. 7, that has nothing to do with the true asymptotic decay rate of the field. Notice, that also the $\ell = 4$ is excited, but at a negligible level. Higher (even) modes are also excited, but not shown in Fig. 10.

In view of the arbitrariness in the slope as calculated over some finite range, it appears that a better way to

evaluate the slope is through its local value, the *local power index* defined by $n(t) := -\dot{\psi}t/\psi$ [8]. Even plotting the local power index as a function of the time could be misleading, as is evident from Figs. 11 and 12: notice how the bold solid curve appears to approach a constant value for low values of t . Indeed, changing the initial conditions, one can make the local power index have an arbitrarily protracted intermediate value.

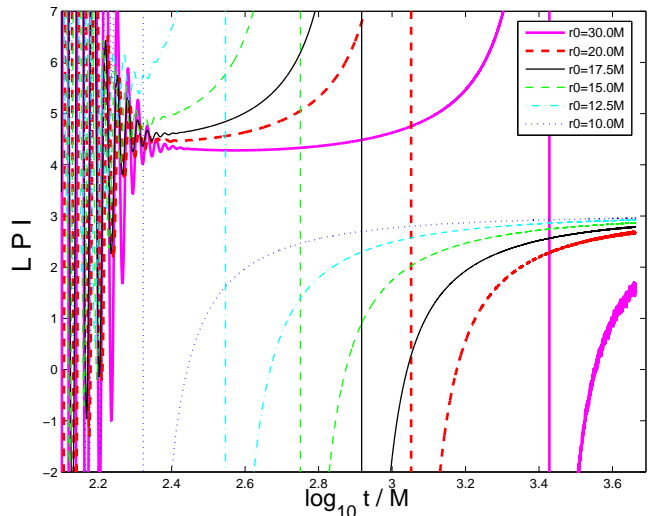


FIG. 11: Local power index (LPI) as a function of t for the same data as in Fig. 9 for the $\ell = 0$ Boyer–Lindquist multipole mode.

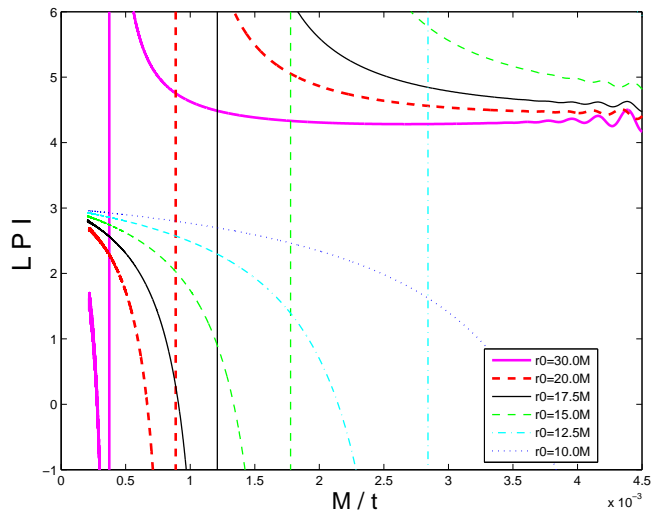


FIG. 12: Same as Fig. 11, but presented as a function of M/t .

How can then one distinguish an arbitrarily protracted intermediate behavior from the true asymptotic behavior? The key point in distinguishing the true asymptotic tail from an intermediate one is to consider the asymptotic behavior of the local power index. As shown in [10],

the asymptotic behavior of the local power index is

$$n(t) = n_\infty + n_1 (M/t) + \dots \quad (2)$$

One should therefore test how well the fit of $n(t)$ as a function of M/t improves with t . Loosely speaking, intermediate regions, like those seen in Fig. 12, will generally yield fits that deteriorate with time, until the true asymptotic regime is reached. How should this criterion be applied in practice? A *necessary condition* is that the ansatz (2) is satisfied *locally*. Specifically, Fig. 13, displays the squared correlation coefficient $1 - R^2$ for constant duration intervals (of ten equally spaced in time values of the local power index). In practice, we choose two sets of data differing only in the location of the initial data pulse, so that one has a protracted intermediate tail, and the other arrives quickly at the asymptotic regime. Indeed, not only does the squared correlation coefficient indicate only relatively poor agreement with the ansatz (2) for the intermediate tail, it also fails to improve at later times. In contrast, at the true asymptotic regime, the squared correlation coefficient approaches unity consistently. We are therefore motivated to introduce the following definition:

Definition: The local power index satisfies the ansatz (2) *locally* if the squared correlation coefficient for fitting the local power indices of constant duration intervals to the ansatz (2) approaches unity as t increases.

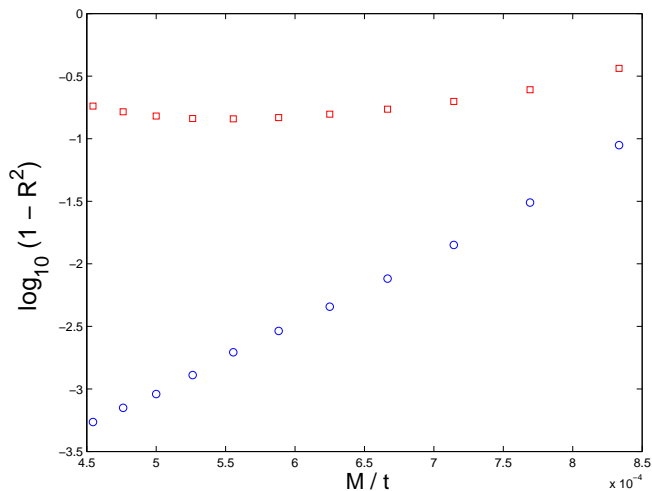


FIG. 13: Dependence of the squared correlation coefficient R^2 on the *local* temporal location of an interval of constant lapse (lasting $1000M$). Data are taken for the same initial data as in Fig. 9. For both cases the data correspond to the squared correlation coefficient of ten evenly spaced (in t/M) values of the local power index (with increments of $100M$) ending at the value shown, fitted to the ansatz (2): Squares (\square) correspond to data for $r_0 = 30M$, and circles (\circ) to $r_0 = 10M$.

The local satisfaction of the ansatz (2) is only a necessary condition for the true asymptotic tail, because in practice we can only examine numerically finite time values. Indeed, this is the very reason why misidentifying

an intermediate tail as an asymptotic one is a problem in the first place. Perhaps not surprisingly, one can find intermediate tails for which the ansatz (2) appears to be satisfied locally, but is violated *globally* in the following sense.

Definition: The local power index satisfies the ansatz (2) *globally* if the squared correlation coefficient for fitting the local power indices of consecutively longer intervals to the ansatz (2) starting from an arbitrary (late) time approaches unity as t increases.

In Fig. 14 we show the local satisfaction but global violation of ansatz (2) for an intermediate tail (upper panel (14A)), and their simultaneous satisfaction for the asymptotic tail (lower panel (14B)).

We are therefore motivated to propose the following as a criterion for distinguishing intermediate from asymptotic tails:

A criterion for identification of the asymptotic tail: The tail is asymptotic if the ansatz (2) is satisfied simultaneously both locally and globally.

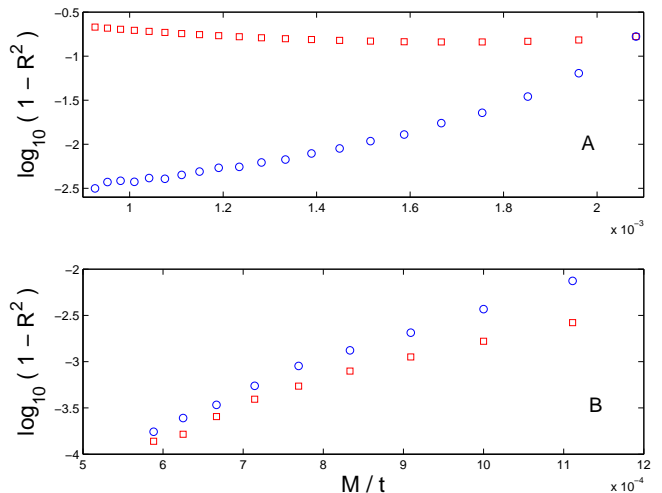


FIG. 14: Dependence of the squared correlation coefficient R^2 on a *global* temporal interval. Upper panel (A): behavior of an intermediate tail. Lower panel (B): behavior of an asymptotic tail. In both panels the local satisfaction of ansatz (2) is shown with circles (\circ), and the global violation (A) or satisfaction (B) of the same ansatz is shown with squares (\square). Initial data are centered on $r_0 = 30M$ (same as in Fig. 9). Data for the upper panel (A) correspond to five evenly spaced (in t/M) values of the local power index (with increments of $30M$) ending at the value shown (local) and appropriately many values with the same spacing (starting at $t = 360M$) and ending at the shown time. Data for the lower panel (B) correspond to five evenly spaced (in t/M) values of the local power index (with increments of $100M$) ending at the value shown (local) and appropriately many values with the same spacing (starting at $t = 500M$) and ending at the shown time.

While figures such as Fig. 7 or the upper panel of Fig. 8 may lead to a misidentification of an intermediate tail as an asymptotic one, we believe that our criterion will expose an intermediate tail as such, and correctly identify

asymptotic tails.

V. POISSON DATA

Poisson has made the argument that if the initial data are in so-called “spherical coordinates,” rather than in Boyer–Lindquist coordinates, which Poisson calls “spheroidal,” mode evolution is changed [6]. In particular, Poisson proposes that in Kerr spacetime such initial data lead to late-time tails according to the prediction by Hod [7]. In a spacetime with global weak curvature (no black hole), Poisson data lead to tail indices similar to Hod’s. This is surprising, as Hod’s results are clearly wrong for the Kerr spacetime that they were derived for. Clearly, the assumption of globally weak curvature affects the tails, and shifts them from their Kerr values to those reported by Poisson. This could be the case if the field reflects off the regular center in the Poisson spacetime, so that the leading order part of the field (in t^{-1}) is cancelled out and one is left with the next order in t^{-1} , or if the monopole part of the field is canceled after the reflection, leaving only the dipole and higher moments present [9]. As the Kerr tail indices were found in [4], the following question arises: what are the tail indices for “pure Poisson” data in a Kerr spacetime? Specifically, if one sets at $t = 0$ a pure $\ell = 4$ mode with respect to the Poisson “spherical” coordinates, does the late time tail decay as $1/t^3$ as predicted by [4], or as $1/t^5$ as predicted by [6] (and also by [7])? As we are showing here, the answer is clearly $1/t^3$.

Initial data that describe a “pure Poisson” mode are a linear combination of Boyer–Lindquist modes, as one may expand such a mode in the function space of Boyer–Lindquist spherical harmonics. Therefore, one may use a code in which the wave equation is written in Boyer–Lindquist coordinates to simulate the evolution of a “pure Poisson” mode, if one writes the initial data as the appropriate linear combination of Boyer–Lindquist modes. This may be done as follows: Denote the Boyer–Lindquist coordinates as $\hat{r}, \hat{\theta}$ and the Poisson “spherical” coordinates as $\tilde{r}, \tilde{\theta}$. As shown in [6], the coordinate transformation is

$$\tilde{r} = \sqrt{\hat{r}^2 + e^2 \sin^2 \hat{\theta}} \quad (3)$$

$$\cos^2 \tilde{\theta} = \frac{\hat{r}^2 \cos^2 \hat{\theta}}{\hat{r}^2 + e^2 \sin^2 \hat{\theta}}, \quad (4)$$

where e is a measure of the “ellipticity” of the Boyer–Lindquist coordinates, which in practice equals the Kerr black hole’s spin a . To specify a “pure Poisson” mode, we take the field to be

$$\begin{aligned} \psi_\ell|_{t=0} &= \tilde{C}_\ell(\tilde{r}) P_\ell(\cos \tilde{\theta}) \\ &\equiv A \exp\left(-\frac{(\tilde{r} - \tilde{r}_0)^2}{2\tilde{\lambda}^2}\right) P_\ell(\cos \tilde{\theta}), \end{aligned} \quad (5)$$

after choosing the radial function to be a gaussian of width $\tilde{\lambda}$ centered on \tilde{r}_0 . The initial “pure Poisson” field

$\psi_\ell|_{t=0}$ can be expanded in the function space of Boyer–Lindquist Legendre polynomials as

$$\psi_\ell|_{t=0} = \sum_{\ell'=0}^{\infty} \ell \hat{C}_{\ell'}(\hat{r}) P_{\ell'}(\cos \hat{\theta}). \quad (6)$$

As shown in [6], the functions $\ell \hat{C}_{\ell'}(\hat{r})$ are complicated. (In fact, only the coefficients for the *inverse* transformation are found in [6] (for $\ell = 4$ and $\ell' = 0$) as a power series in the “ellipticity” e .) In Fig. 15 we show the functions $\tilde{C}_4(\tilde{r})$, and ${}_4\hat{C}_{\ell'}(\hat{r})$ for $\ell' = 0, 2, 4$ (in general, these functions are non-vanishing for all values of ℓ' , respecting the parity symmetry), for a high value for the “ellipticity,” specifically for $e = 0.995M$. To complete the initial data problem, we also need to specify at $t = 0$ the time derivative of the field. It is (arbitrarily) chosen so that the field “momentum” $\Pi := \partial_t \psi + b \partial_{\hat{r}_*} \psi = 0$, where $b = (\hat{r}^2 + a^2)/\hat{\Sigma}$, $\hat{\Sigma} = (\hat{r}^2 + a^2)^2 - a^2 \hat{\Delta} \sin^2 \hat{\theta}$, and $\hat{\Delta} = \hat{r}^2 - 2M\hat{r} + a^2$ (for details see, e.g., [13]).

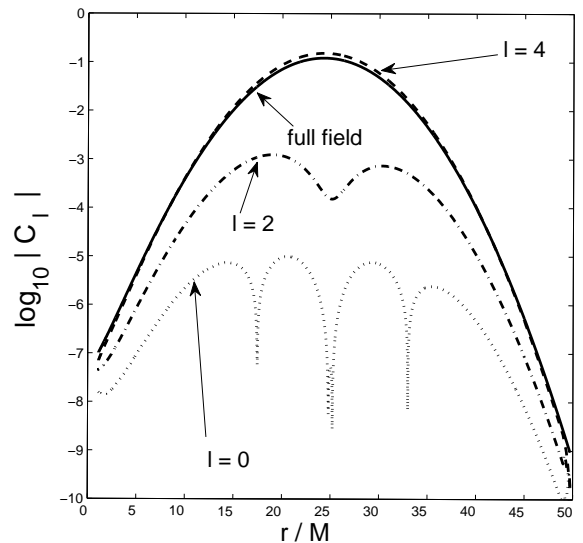


FIG. 15: A scalar field “pure Poisson” $\ell = 4$ mode, $\tilde{C}_4(\tilde{r})$ (solid curve), and its projections on Boyer–Lindquist ℓ modes ${}_4\hat{C}_{\ell'}(\hat{r})$: dashed ($\ell' = 4$), dash-dotted ($\ell' = 2$), and dotted ($\ell' = 0$). Here, $a/M = 0.995$. The initial data radial profile is a gaussian with $\tilde{r}_0 = 25M$ and $\tilde{\lambda} = 4M$. The abscissa is \tilde{r}/M or \hat{r}/M as is appropriate.

Figure 16 suggests that the tail field drops off as $1/t^3$ for a scalar field with initial data that are a “pure Poisson” $\ell = 4$ mode in agreement with our expectations. Below, we show this to be the case more precisely, using the criterion based on simultaneous local and global behavior of the local power index. Comparison of the evolution of the evolution of the “pure Poisson” $\ell = 4$ mode with the evolution of its Boyer–Lindquist $\ell' = 4$ projection suggests that the monopole projection $\ell' = 0$ at the initial time is important at late times. The $\ell' = 0$ mode is being excited during the evolution also when it is not present

at the initial time, and eventually it dominates the field at late times. However, the generated $\ell' = 0$ mode starts dominating the total field only at a later time, as its amplitude is lower than that of the monopole part of the full $\ell = 4$ mode. The latter mode includes a monopole component already at the initial time, and this part of the field starts dominating the total field at an earlier time than the monopole component that is excited. For this reason the asymptotic $\ell = 4$ mode is much stronger than the asymptotic tail of initial data that include only the $\ell' = 4$ projection of the $\ell = 4$ mode, even though at the initial time they are almost identical, as can be seen in Fig. 15.

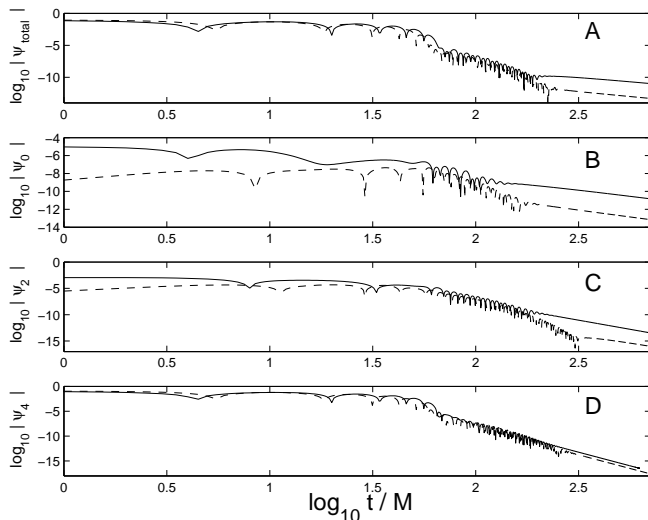


FIG. 16: Time evolution of a “pure Poisson” $\ell = 4$ mode (panel A), and its Boyer–Lindquist $\ell' = 0, 2, 4$ modes (panels B, C, and D, respectively) (solid curves), and the evolution of the Boyer–Lindquist $\ell' = 4$ projection of the “pure Poisson” mode and its Boyer–Lindquist projections (dashed curves). Here, $a/M = 0.995$. The initial data are those of Fig. 15.

To show that indeed the late-time tail is dominated by the evolution of the $\ell' = 0$ projection of the original “pure Poisson” $\ell = 4$ mode at $t = 0$, we present in Fig. 17 the evolution of this mode. Comparison with Fig. 16 indeed shows that the late time field of the full $\ell = 4$ mode is dominated by the evolution of its monopole projection, not the monopole mode that is excited during the evolution because of mode coupling.

In Fig. 18 we show the behavior of the local power indices for the full field of the “pure Poisson” $\ell = 4$ mode, and for its monopole $\ell' = 0$ projection. Figure 18 strongly suggests that the full field, and also the monopole projection, drop off at late times as $1/t^3$. Indeed, the tail seen in Figs. 17 and 18 is asymptotic, and the local power index satisfies the ansatz (2) both locally and globally simultaneously. As noted in [6], it is not surprising that starting with the initial data of a $Y_{\ell=4}^{m=0}$ mode, the $Y_{\ell=0}^{m=0}$ mode is excited. Figure 18 (in conjunction with the conclusion that the tail is asymp-

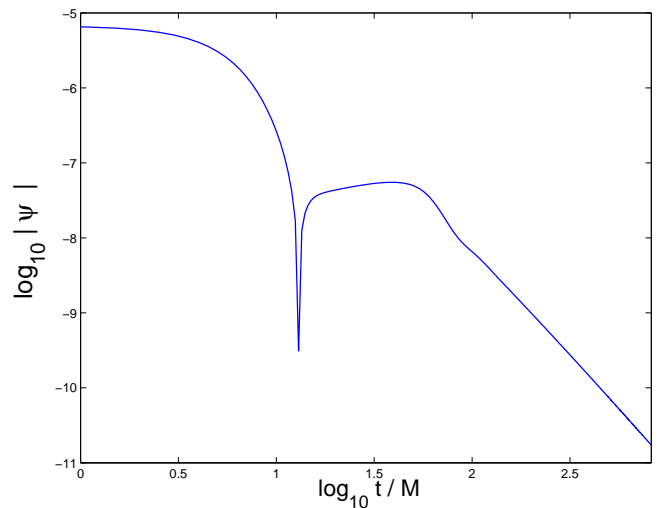


FIG. 17: Time evolution of the Boyer–Lindquist $\ell' = 0$ projection of the “pure Poisson” $\ell = 4$ mode. The initial data are those of Fig. 15.

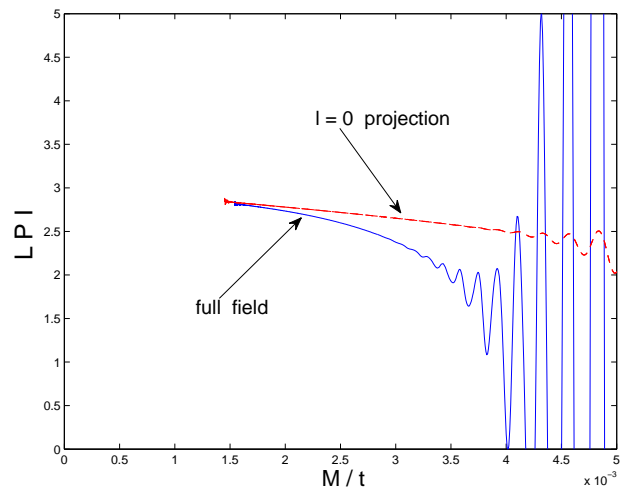


FIG. 18: The local power index as a function of t^{-1} for the “pure Poisson” mode $\ell = 4$ (solid curve) and for its $\ell' = 0$ Boyer–Lindquist projection (dashed curve). The initial data are those of Fig. 15, and the field evolution is presented in Fig. 16.

otic) shows that when starting with a “pure Poisson” mode, the excited monopole mode is insignificant for the asymptotic tail problem, as it is swamped by the evolution of the monopole projection of the initial data. Above, we showed that starting with initial data of a pure Boyer–Lindquist $\ell = 4, m = 0$, the late time tail drops off according to t^{-3} . In that case, there is no monopole field present at $t = 0$, and all the monopole field present at late times is due to the excitation of the $\ell = 0$ mode due to mode coupling. That excited mode and also the monopole mode existing at the initial time drop off as t^{-3} , because an $\ell = 0$ mode behaves like any

other monopole mode, and has no memory of its history and how it came about, whether through excitation or because it was present in the initial data.

Most importantly, we chose the initial data to be a pure spherical harmonic mode in the so-called “spherical” coordinates. The late time tail still decays according to the conclusions of [4], that is, the late time tail drops off as $t^{-(2\bar{\ell}+3)}$, where $\bar{\ell}$ is the least value of ℓ that is not disallowed (which may equal m or $m + 1$ depending on whether $\ell + m$ is even or odd, respectively). In the case presented, as the initial mode is azimuthal, the asymptotic tail drops off as t^{-3} . In [6] a surprise is voiced that the $Y_{\ell=m}^m$ mode (for the even case) presumably does not drop off as $t^{-(2m+3)}$. There is no reason to be surprised: this mode does decay according to sound physical expectations. The contention of [6]—when carried over to the Kerr case—that the late time tail is extremely sensitive

to the form of the initial data is shown here to be unsubstantiated. Specifically, all initial data sets of compact support evolve to similar late time tails.

acknowledgments

The authors wish to thank Richard Price for many invaluable discussions. Early work on this problem was done with Elspeth Allen at the University of Utah. LMB is supported in part by NASA/GSFC/EPSCoR grant No. NCC-580 and by NASA/Stennis/EPSCoR grant No. NNX07AL52A. GK is grateful for research support from the UMD College of Engineering RSI Fund and SCEA. Many of the simulations were performed on NSF’s TeraGrid infrastructure (under grant number TG-PHY060047T) and the HPC Consortium’s facilities.

-
- [1] R.H. Price, Phys. Rev. D **5**, 2419 (1972).
 - [2] J. Bičák, Gen. Relativ. Gravitation **3**, 331 (1972).
 - [3] C.J. Blaksley and L.M. Burko, Phys. Rev. D (in press) [arXiv:0710.2915].
 - [4] L.M. Burko and G. Khanna, Phys. Rev. D **67**, 081502(R) (2003).
 - [5] W. Krivan, Phys. Rev. D **60**, 101501 (1999).
 - [6] E. Poisson, Phys. Rev. D **66**, 044008 (2002).
 - [7] S. Hod, Phys. Rev. D **61**, 024033 (2000); **61**, 064018 (2000).
 - [8] L.M. Burko and A. Ori, Phys. Rev. D **56**, 7820 (1997).
 - [9] R.J. Gleiser, R.H. Price, and J. Pullin, arXiv:0710.4183.
 - [10] A.Z. Smith and L.M. Burko, Phys. Rev. D **74**, 028501 (2006).
 - [11] M.A. Scheel, A.L. Erickcek, L.M. Burko, L.E. Kidder, H.P. Pfeiffer, and S.A. Teukolsky, Phys. Rev. D **69**, 104006 (2004).
 - [12] W. Krivan, P. Laguna, P. Papadopoulos, and N. Andersson, Phys. Rev. D **56**, 3395 (1997).
 - [13] E. Pazos-Ávalos and C.O. Lousto, Phys. Rev. D **72**, 084022 (2005).